Heliyon 6 (2020) e05610

Contents lists available at ScienceDirect

Heliyon

journal homepage: www.cell.com/heliyon

Research article

Flux model development and synthesis optimization for an enhanced GO embedded nanocomposite membrane through FFD and RSM approach

Mohamad Syafiq Abdul Wahab, Sunarti Abd Rahman *, Rozaimi Abu Samah

Department of Chemical Engineering, College of Engineering, Universiti Malaysia Pahang, Lebuhraya Tun Razak, 26300 Gambang, Kuantan, Pahang, Malaysia

ARTICLE INFO

Keywords:
Chemical engineering
Membrane
Transport process
Computer-aided engineering
Films
Thin film
Nanomaterials
Composite film
Hydrophilic enhancement
ANOVA
Optimization

ABSTRACT

A two-level full factorial design was used to analyze several factors involved in PSF–GO–Pebax thin film nanocomposite membranes development. Permeate flux was chosen as a single response for four possible factors: Pebax selective layer concentration, amount of GO load to Pebax selective layer, Pebax–GO selective layer thickness, and amount of GO load to PSF substrate. The study is aimed at factors interaction and contribution towards the highest permeation flux via FFD and RSM approach. R^2 obtained from the ANOVA is 0.9937 with Pebax concentration as the highest contributing factor. Pebax concentration–amount of GO load to PSF substrate is the only interaction contributing to the highest flux. A regression analysis concluded the study with model development and an optimized condition for the membrane design.

1. Introduction

There are numerous design techniques in design of experiment (DOE), such as Box–Behnken design (BBD), full factorial design (FFD), and central composite design (CCD). FFD can simulate a wide range of factors with its discrete levels. The combination of factors and level will determine the total number of experiments needed to be carried out. A two-level experiment with three independent variables could be written as 2^3 design, which makes up a total of 16 runs. In comparison, a three-level experiment with three independent variables could be written as 3^3, totaling 27 runs. The differences between both design arrangements are tabulated in Tables 1 and 2.

For two-level design (Table 1), factors to be defined (numeric or categoric) will be the low (−1) and high (1) for each of the variables involves, while in three-level design (Table 2), factors to be defined will start from the lowest (0), intermediate (1), and the highest (2). For screening purposes, two-level design is sufficient considering that further optimization will be carried out with center points (repetition points), and it is less time-consuming to reach the same objective. On the other hand, BBD is almost the same as 3^3 FFD design but leaning towards RSM rather than a screening method. RSM aims for optimum process condition and closely studies the weakest points in experiment design, process, and product development. BBD is a good design when the optimum point is expected to lie in between the factors range. Unlike CCD, this method does not contain an embedded factorial design; the treatment is only at the midpoints. CCD offers a robust design with an extra star point, denoted as alpha, so that it can navigate beyond the level. A design containing two levels (+1, −1), center point (0), and axial or star point (+α, −α) makes this design a flexible five-level on every edge of the process space. The total number of runs is manipulated by the repetitive center points as given by Eq. (1):

$$N = 2^n + 2n + C \quad (1)$$

where N is the number of runs, n is the number of independent factors (≥2) involved in the design, and C is the center points set between 2 and 6.

This RSM optimization method is widely used in operation and process-based such as desalination, membrane distillation [1, 2], pervaporation [3], gas separation [4], and reverse osmosis owing to its reliabilities, ease of operation, and reproducibility of models parameter for an attractive application and scalable usage. Every design comes with its added value and disadvantages depending on experimental needs. Many studies have shown the ability of FFD in minimizing the number of runs over one-factor-at-a-time (OFAT) techniques [1, 5]. For the same amount

* Corresponding author.
E-mail address: sunarti@ump.edu.my (S. Abd Rahman).

https://doi.org/10.1016/j.heliyon.2020.e05610
Received 4 November 2020; Received in revised form 11 November 2020; Accepted 23 November 2020

Table 1. FFD 2^3 design table.

Run	Factor A	Factor B	Factor C
1	−1	−1	−1
2	1	−1	−1
3	−1	1	−1
4	1	1	−1
5	−1	−1	1
6	1	−1	1
7	−1	1	1
8	1	1	1

Table 2. FFD 3^3 design table.

Factor B	Factor C	Factor A		
		0	1	2
0	0	000	100	200
0	1	001	101	201
0	2	002	102	202
1	0	010	110	210
1	1	011	111	211
1	2	012	112	212
2	0	020	120	220
2	1	021	121	221
2	2	022	122	222

Table 3. Fractional factorial design of PSF-GO-Pebax thin film nanocomposite.

Run	X_1	X_2	X_3	X_4
	A: Pebax concentration (wt %)	B: GO dispersed in Pebax (wt %)	C: GO dispersed in PSF (wt %)	D: Pebax–GO coating layer
1	1	0.5	0.4	1
2	3	0.5	0.4	3
3	3	0.5	0	1
4	1	0	0.4	1
5	3	0	0.4	3
6	3	0.5	0	3
7	1	0	0	3
8	3	0	0	3
9	1	0	0	1
10	3	0	0.4	1
11	3	0.5	0.4	1
12	1	0	0.4	3
13	1	0.5	0	1
14	1	0.5	0	3
15	1	0.5	0.4	3
16	3	0	0	1

of accuracy, FFD would take less time compared to OFAT. In an environment where too many factors to be considered, FFD could be a screening method to eliminate factors that contribute less toward the final response. This technique is superior compared to OFAT because of the provided interaction variables that contribute to the response and can be assessed in eliminating less responsive factors. A study applied a three-level FFD in designing hollow fiber membranes for membrane distillation where the observed responses in experimental design are in agreement with those predicted by the model [6]. For studies with more factors, the number of experiments can be reduced by applying a fractional factorial design, 2^{k-m}, where k is the number of factors and m is the size of the fraction of the full factorial ranging from 1 to 16 depending on the k involved, and k−m must be between 2 and 9 to satisfy the original FFD. Another study managed to reduce the number of experiments from 128 to only eight runs in designing poly(vinylidene fluoride-co-hexafluoropropylene), PVDF-HFP with polyethylene glycol, PEG additive hollow fiber membranes involving seven factors [7]. It proves that FFD is reliable to be applied in membrane development.

This paper introduces the combined usage of FFD and RSM in experimental design for multiple variables, and it is suspected to influence the outcome and estimate the optimum design condition. The validity of the predicted point from a three-dimensional (3D) plot can be tested experimentally, where the error margin of less than 5% is desired [5]. Applying either of these methods in DOE could generate a better prediction, minimize mass production cost, and increase process efficiency [8].

Table 4. Optimization of film development via CCD.

Run	A: Pebax concentration, (wt %)	B: GO dispersed in Pebax, (wt %)
1	3.00	0.40
2	3.00	0.26
3	1.59	0.40
4	3.00	0.40
5	4.41	0.40
6	4.00	0.50
7	2.00	0.30
8	3.00	0.40
9	3.00	0.54
10	4.00	0.30
11	3.00	0.40
12	3.00	0.40
13	2.00	0.50

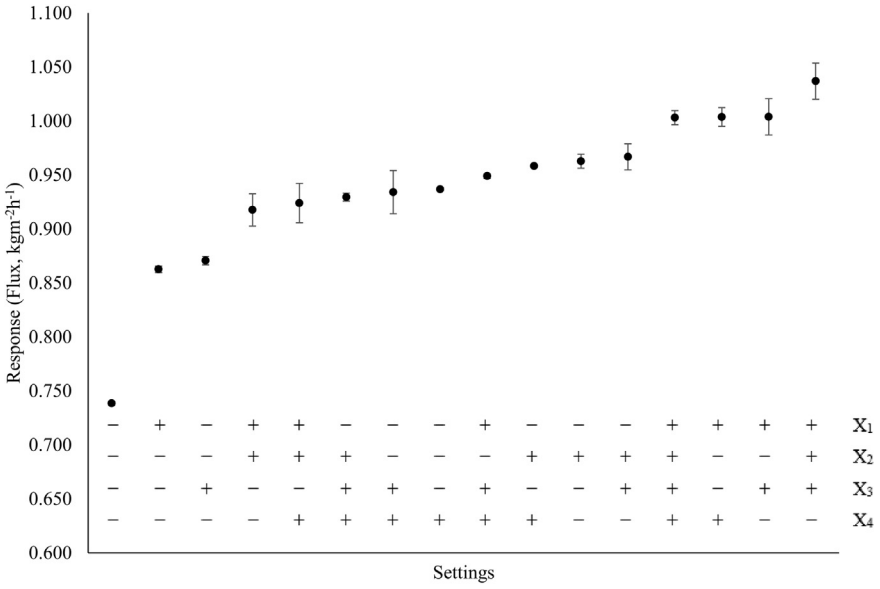

Figure 1. Ordered data plot for each setting of each factor.

2. Experimental

2.1. Materials

Polysulfone (PSF), with a density of 1.23 g/cm^3, 79° film contact angle, a glass transition temperature of 185 °C, and an average molecular weight of 45,000–55,000 g/mol, was supplied by Gardner Global. Polyether block amide (Pebax) was provided by Arkema France under the trade name Pebax MH 1657. Graphene oxide (GO, 763713-1G) was supplied by Sigma Aldrich. The solvents used in this study, isopropyl alcohol (IPA) with 99.98% purity was supplied by HmbG Chemicals, and 99.9% ethanol and dimethylformamide (DMF) were provided by Sigma Aldrich.

2.2. Composite film development

The PSF substrate was prepared via the dry/wet phase inversion of 15 wt % PSF in 85 wt % dimethylformamide at 90 °C. The factorial study also includes 0–0.4 wt % GO dispersed into the PSF dope solution. The bubble-free solution was then cast on a glass plate, instantly immersed in a water bath for 1 h, and dried at room temperature for 24 h. The selective dense layer was made up of 1–3 wt % Pebax 1657, and 0–0.5 wt % GO was dissolved in 70/30 ethanol/water at 80 °C for 3 h. The selective solution was poured on the PSF substrate (1–3 layers), and it was oven-dried at 60 °C for 24 h. The factorial range was obtained from our previous OFAT work [9]. A two-level FFD (2^4) approach was applied to this study, and the experimental design for this experiment is presented in Table 3.

After evaluating the response, the two most contributed variables (factors) were taken further for optimization. CCD aided by Design Expert 7.0 (Stat-Ease, Minneapolis) was employed with a quadratic model, 13 runs, five center points, one replication of factorial and star points, and rotatable with an alpha of 1.41421. The summary of the experimental run is given in Table 4.

2.3. IPA dehydration

A simple lab scale pervaporation system consisted of a 1 L feed tank, a fixed flow pump of 1 L/min, a 0.00385 m^2 membrane cell, an evacuated cold trap jacketed with 10 °C chilled water, and a 55 mmHg vacuum pump on the permeate side was set up. Permeate was collected and weighed on a Shimadzu AY220 weighing balance. Permeate composition was determined by Atago Pocket refractometer (PAL-37s) and double-confirmed with FTIR absorbance. Flux was chosen as a single response

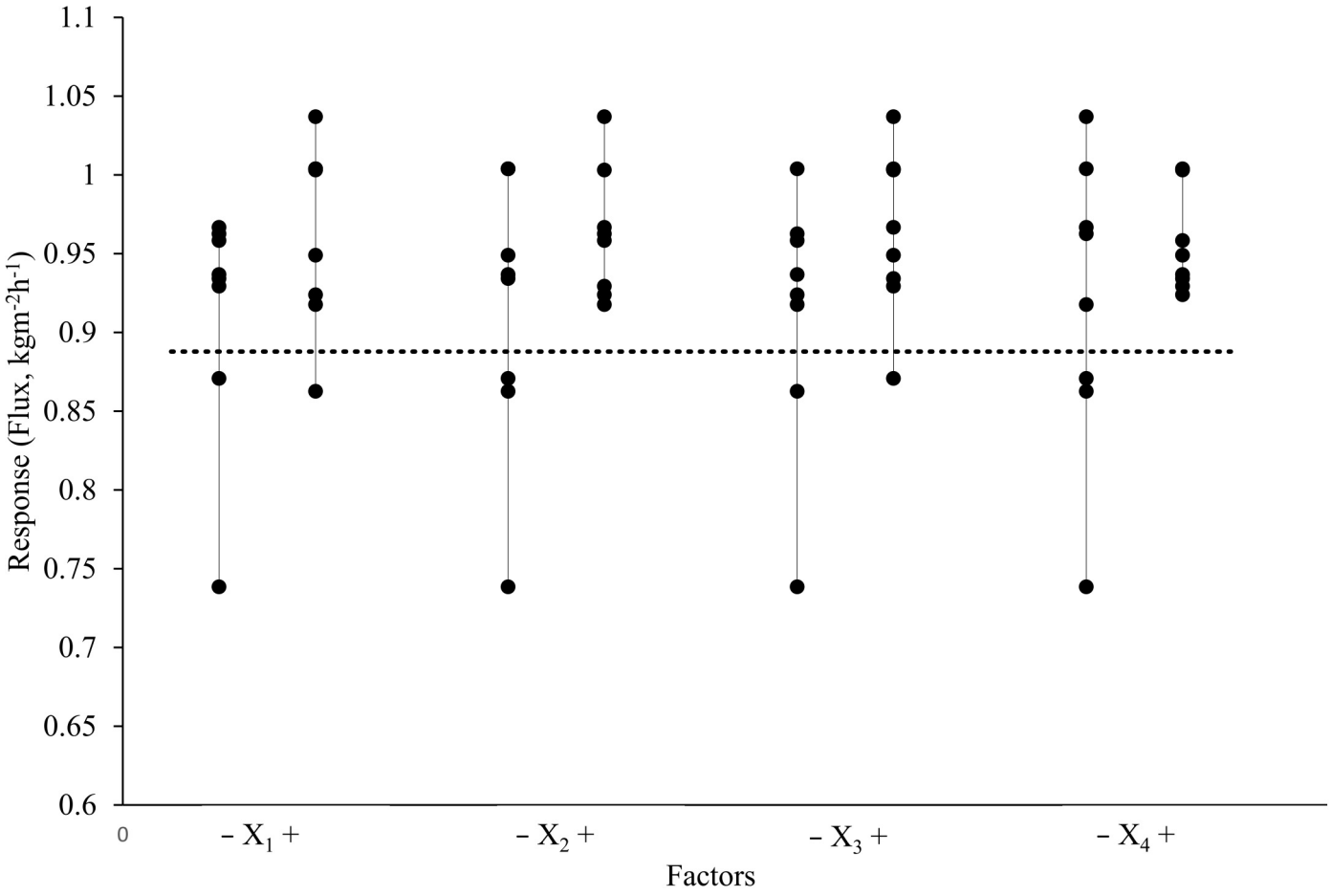

Figure 2. Scattered plot within factors setting.

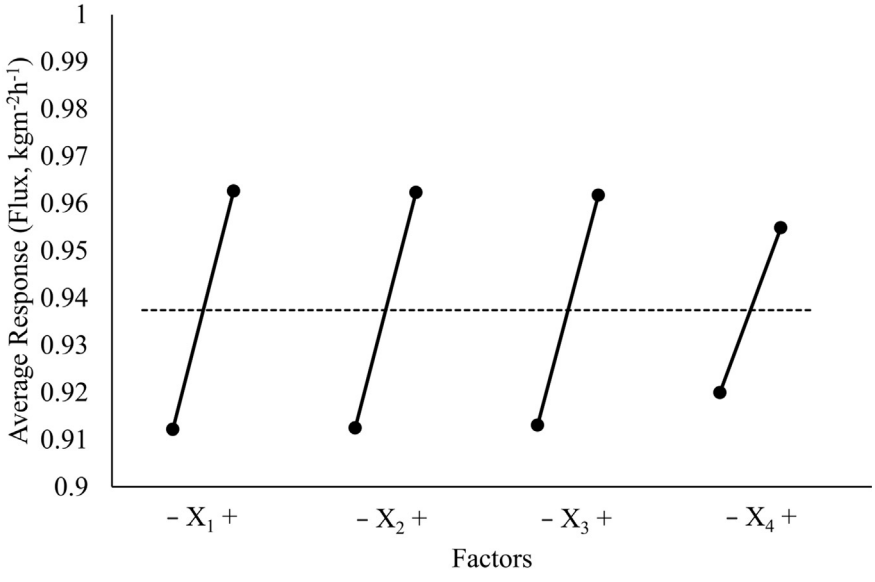

Figure 3. Mean plot of the permeate flux.

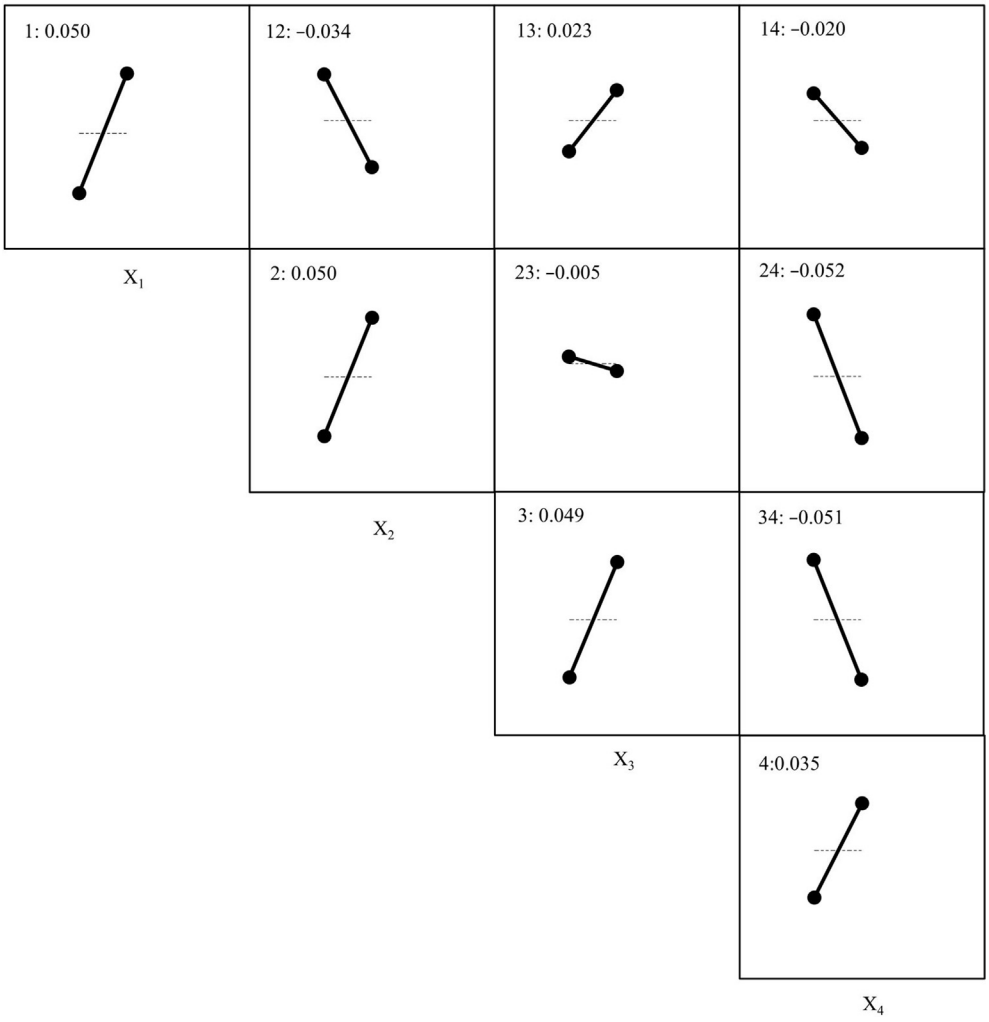

Figure 4. Permeate flux interaction effect matrix.

Table 5. ANOVA of the FFD design.

Source	Sum of squares	Degree of freedom	Mean square	*F* Value	*p*-value Prob > *F*	
Model	0.075	12	6.230×10^{-3}	31.95	0.0078	**significant**
X_1: Pebax concentration (wt %)	0.010	1	0.010	52.20	0.0055	
X_2: GO dispersed in Pebax (wt %)	9.953×10^{-3}	1	9.953×10^{-3}	51.04	0.0056	
X_3: GO dispersed in PSF (wt %)	9.484×10^{-3}	1	9.484×10^{-3}	48.64	0.0061	
X_4: Pebax–GO coating layer	4.868×10^{-3}	1	4.868×10^{-3}	24.96	0.0154	
X_1X_2	4.711×10^{-3}	1	4.711×10^{-3}	24.16	0.0161	
X_1X_3	2.034×10^{-3}	1	2.034×10^{-3}	10.43	0.0482	
X_1X_4	1.619×10^{-3}	1	1.619×10^{-3}	8.30	0.0635	
X_2X_4	0.011	1	0.011	55.78	0.0050	
X_3X_4	0.010	1	0.010	52.32	0.0054	
$X_1X_2X_3$	4.436×10^{-3}	1	4.436×10^{-3}	22.75	0.0175	
$X_1X_2X_4$	2.243×10^{-3}	1	2.243×10^{-3}	11.50	0.0427	
$X_2X_3X_4$	4.154×10^{-3}	1	4.154×10^{-3}	21.30	0.0191	
Residual	5.850×10^{-4}	3	1.950×10^{-4}			
Correlation total	0.075	15				

Table 6. Coefficients of determination.

R^2	0.9922
Adjusted R^2	0.9612
Predicted R^2	0.7792
Adequate precision	24.238

for this study due to IPA contents for each film tested was found to be 0 wt %. The total permeation flux (j) was calculated using Eq. (2).

$$j = \frac{wA}{t} \tag{2}$$

where j is total permeation flux in $kgm^{-2}h^{-1}$, w is the permeate mass in kg, A is the membrane surface area in m^2, and t is the permeation time in h.

3. Results and discussions

3.1. Exploratory data analysis (EDA)

As a preliminary judgment, an exploratory data analysis (EDA) approach was used in assessing all the data. Initially, two questions should be answers from this point; 1- The best setting for the k factors involved, and 2- which are the most critical, and which is not. The variety of data sets often leads to unbalanced judgment in deciding important and unimportant factors, the best setting for each factor involved should satisfy the data, average and predicted data of adequate model and most importantly to maximizing response or in this case, the permeate flux. An ordered data plot of the response against the factors setting is presented in Figure 1.

From Figure 1, an early judgment can be made based on the highest flux and the combination of setting for each k (factors) involved. The best setting for this data set is at 1.037 $kgm^{-2}h^{-1}$, where (X_1, X_2, X_3, X_4) = (+1, +1, +1, −1). The most contributing factors are denoted by the consistency of the setting for that factor at the highest and lowest responses. From this plot, X_1, X_2, and X_3 appeared to repeatedly contribute to half of the highest response with the same setting (5 out of 8). A conclusion cannot be made yet, as there are three most important factors found from the ordered plot. A scattered plot in Figure 2 was constructed to study any outliers within this data set. The best setting for the three most important factors found in the ordered data plot can also be studied. For all data with a shift in position from a positive setting to a negative setting, a factor could be considered important when there is a significant change or variation of response within the setting range. X_1, X_2, and X_3 showed a positive location shift towards maximizing the response.

Between the three factors, X_1 is the least to have overlapping data between the negative (−) and positive (+) setting making it the most important single factor, followed by X_2 and X_3. On the other hand, X_4 has all data overlapping between the setting, making it not important toward the response. The best setting for maximizing the response would be (X_1, X_2, X_3) = (+1, +1, +1), and there are no outliers within this data set. The order of the second and third vital factors cannot be judged merely from this plot due to the degree of overlapping is almost identical. Figure 3 represents the mean plot of the permeate flux for each factor involved. This is an alternative to the one in Figure 2, but it can assess a wide range of factors compared to a scattered plot, which trustable for the first and second most important factors only. An actual ranking of the contribution order of the main factors can be expected.

All factors seem to have a shifted average response from the negative to positive setting, meaning that they might have potential. However, the steepest changes accounted for the most influencing factors. The average response for + X_2 is 0.9623 $kgm^{-2}h^{-1}$ and 0.9617 $kgm^{-2}h^{-1}$ for + X_3, making X_2 coming second after X_1. For the main factor contribution, the list of contributors from the highest to the lowest is X_1, X_2, X_3, and X_4, and the best setting for the factors is at (−) setting, (X_1, X_2, X_3, X_4) = (+1, +1, +1, +1). There is a $2^k - 1 - k$ possible interaction within the experimental design. For this study with k = 4, 11 interactions could be navigated within this data. Only two-factor interactions were studied because it is mostly practical compared to the rest. The number of two-factor interactions can be calculated using Eq. (3).

$$\binom{k}{2} = \frac{k!}{2!(k-2)!} = \frac{k(k-1)}{2} \tag{3}$$

For this data set of k = 4, six two-factor interactions were involved. A set of contribution ranking could be made involving both main factors

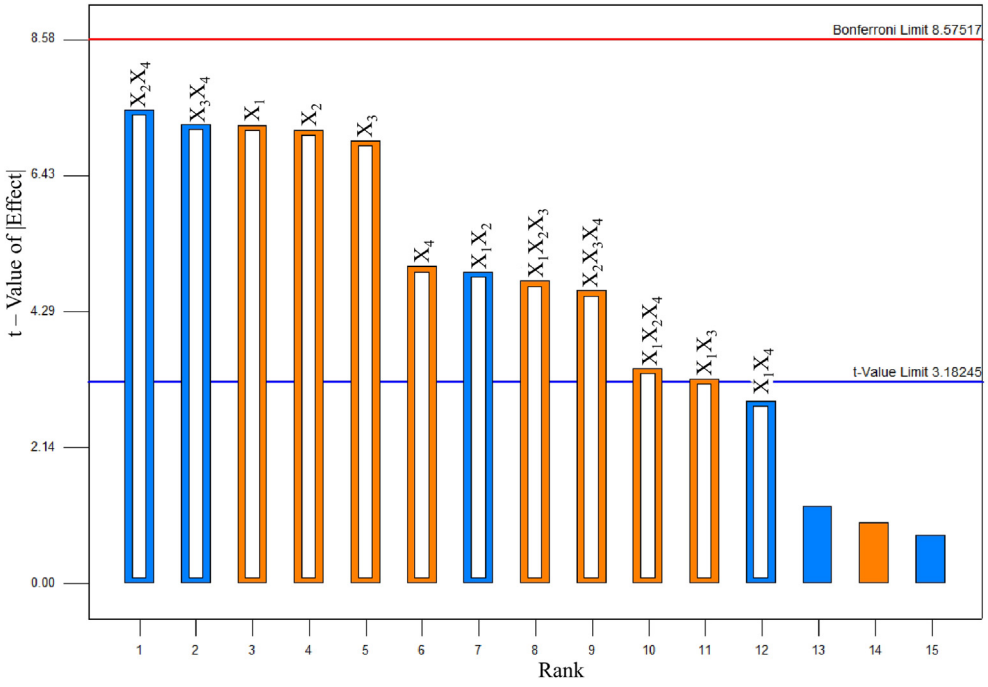

Figure 5. Pareto chart of t-value of main and interaction effects.

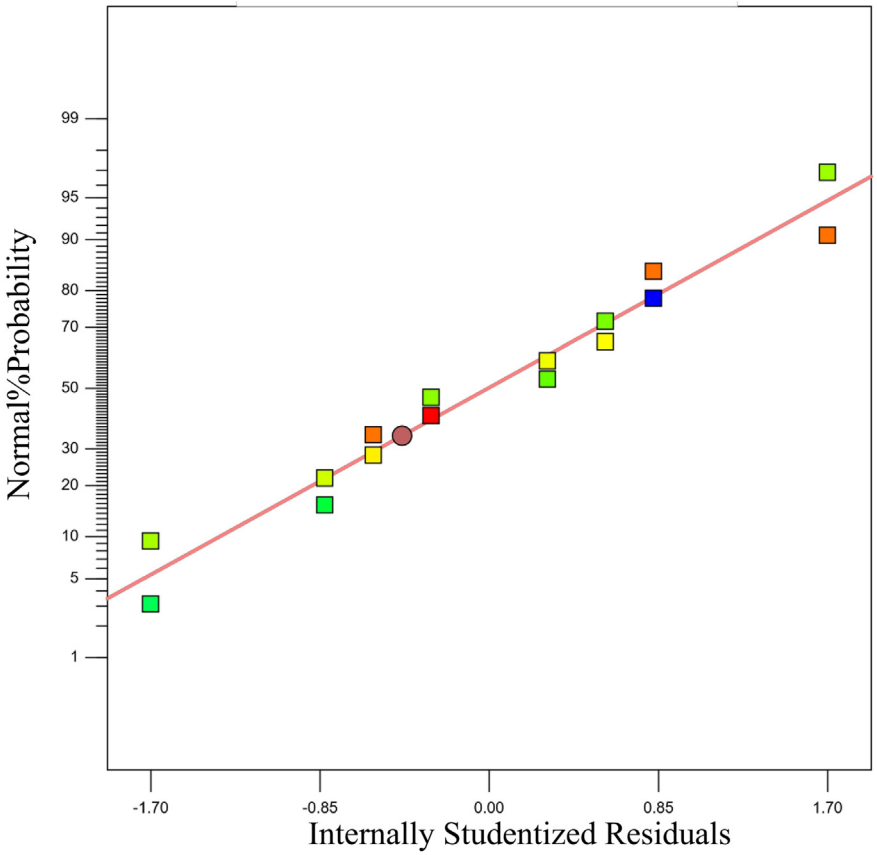

Figure 6. Normal probability against internally studentized residuals.

and interaction. An upper triangular matrix plot consisted of main diagonal factors, and off-diagonal interaction factors is illustrated in Figure 4. All the plots were constructed on the same scale with a common horizontal (two-level setting) and the vertical axis (average responses). The largest shift between the setting defines the importance of the factors. Based on the steepness denoted by the magnitude of the average response different from the changes in setting from negative to positive, a rank of the factors, including the interaction, could be written as follows:

1. X_2–X_4 (−0.052)
2. X_3–X_4 (−0.051)
3. X_1 (0.050)
4. X_2 (0.050)
5. X_3 (0.049)
6. X_4 (0.035)
7. X_1–X_2 (−0.034)
8. X_1–X_4 (−0.020)
9. X_1–X_3 (0.023)
10. X_2–X_3 (−0.005)

There is only one interaction that positively affected the response, which is X_1–X_3. It is relatable how Pebax concentration (X_1) and GO dispersed in PSF support (X_3) are related to one another. Changes in either one positively impacted the other. Both factors introduce more hydrophilic moieties to the film, thus affecting the response.

3.2. Analysis of variance (ANOVA)

Many have used ANOVA in accessing the significant factor and model prediction in parameter analysis for membrane development. Different factors or parameters combinations lead to a different conclusion to minimize or maximize the response. A model fitted with the involved factors can be easily tested based on the regression method. So, response (permeate flux) can be calculated upper hands based on all the factors study within this experiment. The *F*-test through ANOVA analysis was used as a tool for model validation and the adequacy for data judgment. The statistical figures for the permeate flux of the ANOVA analysis are listed in Table 5. The model *F*-value of 31.95 indicates that the model is statistically significant within the design space. It is a ratio of two variances: the model to the residual describing the dispersion of the study data from its mean. The *p*-value of 0.0078 associated with this model development is quite large but still comparable to the set alpha (0.05), so it can be concluded that only 0.78% of the broader data dispersion occurs due to noise. Nevertheless, if the $p > F$-value is smaller than 0.0500, the terms in the models significantly affect the response in which a null hypothesis can be rejected from this point.

The values of R^2 and adjusted R^2 of this model are close at 0.9922 and 0.9612, respectively (Table 6). When R^2 explains how the terms or the scattered data points fit the curve, with 1 is considered to be the best fit, adjusted R^2 works almost the same but it would be the indicator for model reduction. The adjusted R^2 can be calculated using Eq. (4):

$$R^2_{adj} = 1 - \left[\frac{(1-R^2)(n-1)}{n-k-1}\right] \quad (4)$$

where n is the number of points, and k is the number of variables. Adding more terms to a model increases the R^2 approaching 1, but not all terms added are significant. Thus it creates a misleading and imprecise projection. Adjusted R^2 comes in handy by reducing the figures far from R^2 when there are too many independent variables within the model term. Having both values in a regression analysis will prevent overfitting of the model curve. The predicted R^2 for this model is in reasonable agreement with the adjusted R^2. So, this regression model is not only providing an

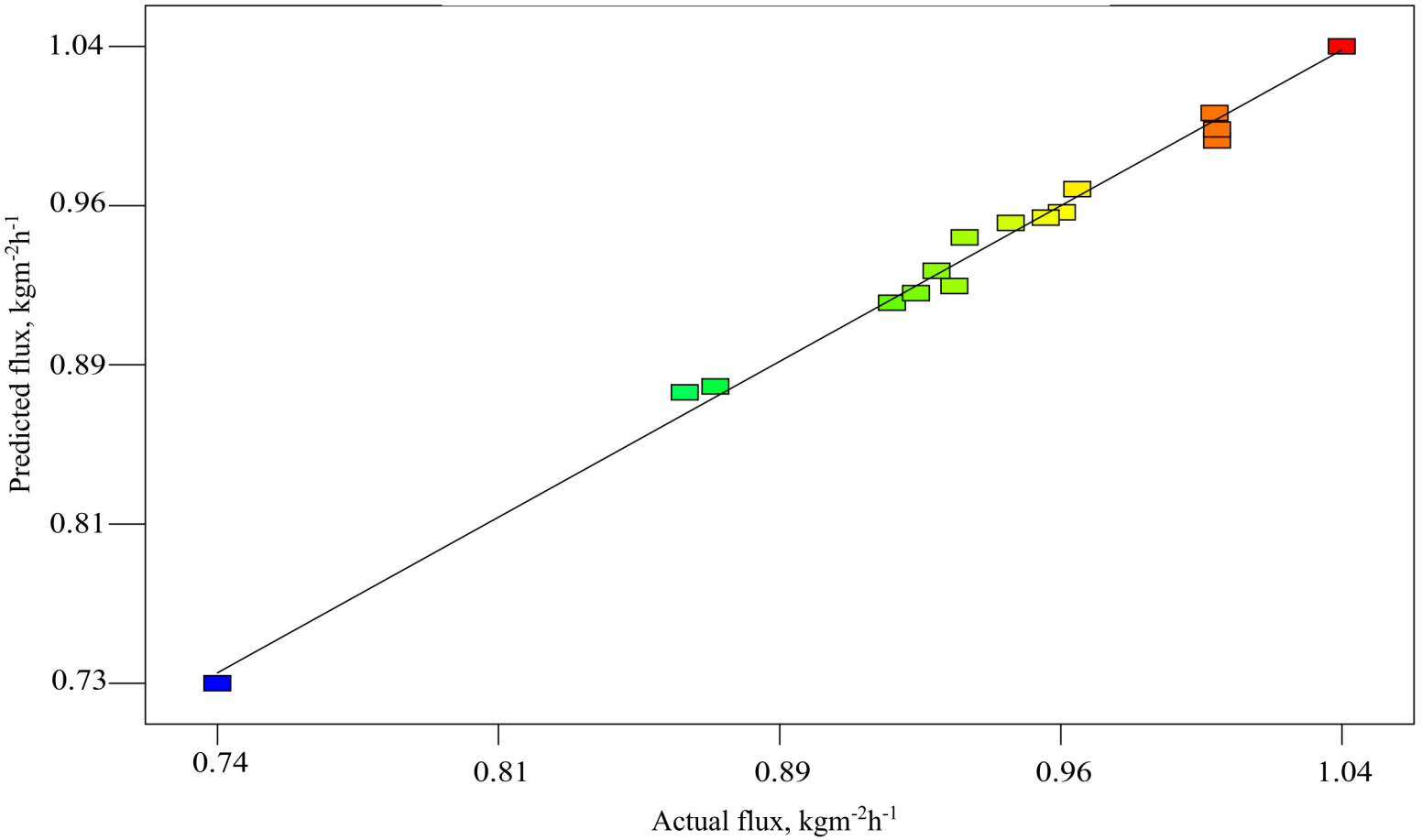

Figure 7. Predicted flux against the actual flux of the developed model.

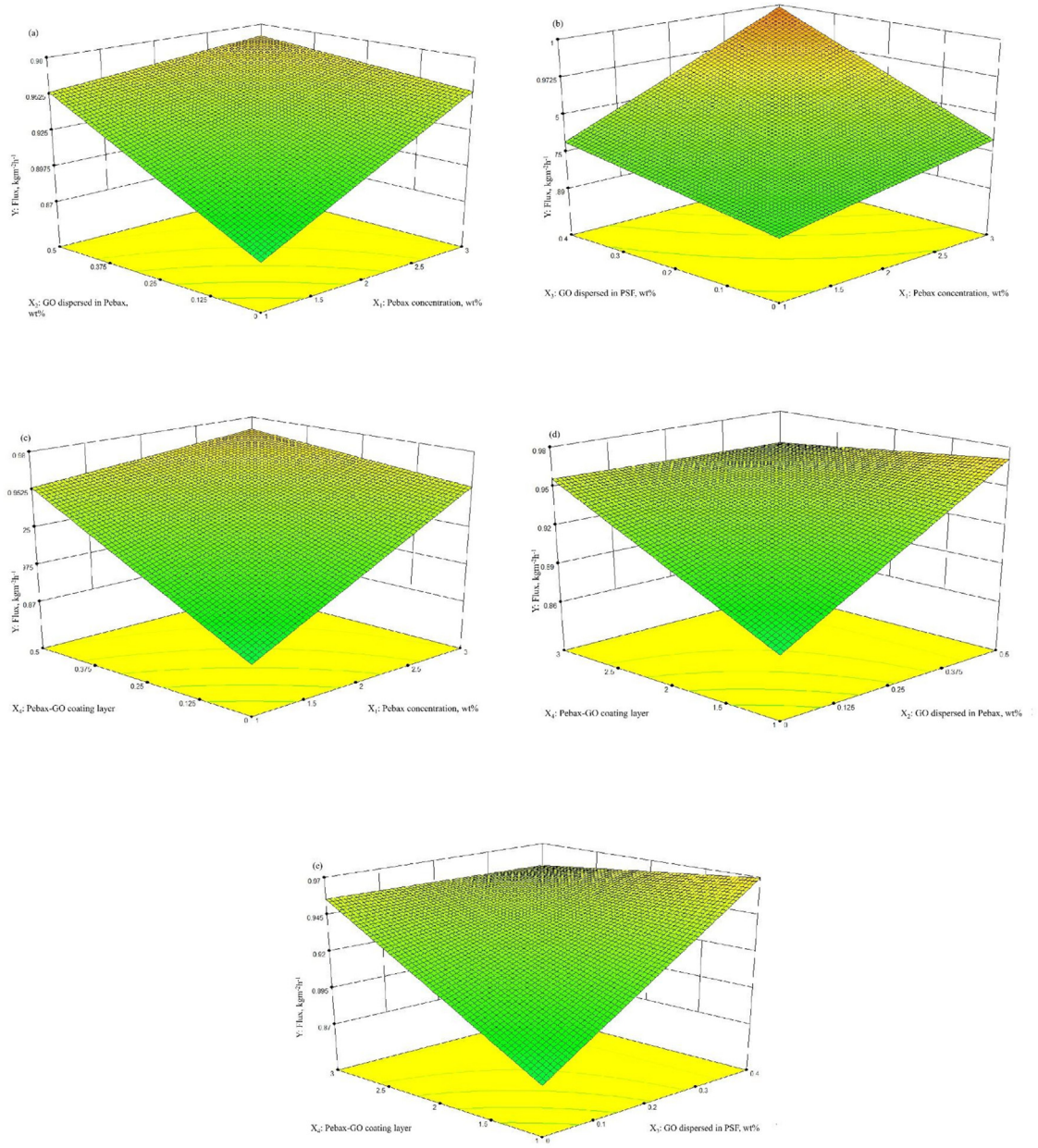

Figure 8. Three-dimensional interaction plots of flux as a function of (a) X_1–X_2, (b) X_1–X_3, (c) X_1–X_4, (d) X_2–X_4, and (e) X_3–X_4.

excellent fit to the existing data point but good enough at making a prediction. The closeness of these two R^2 values gives an insight that the regression model contains an amount of acceptable random noises to the sample. If there is a specific number of random noises occurs in the sample, one could never get a comparable figure of all three R^2 values and the regression model could be overfitting or lack of fit, thus leading to an unusable model. Then, that is where model term reduction should be made. Adequate precision measures the signal-to-noise ratio. It is a comparative figure of predicted value to the average prediction error [10]. A ratio greater than 4 is desirable. The ratio of 24.238 indicates an adequate signal, which means this model can be used to navigate the design space.

A Pareto chart of t-value for each factor was tabulated into a ranking bar in Figure 5. This chart will give a clear insight into which parameter should be kept or ignored for further optimization. Positive and negative effects toward maximizing the permeate flux were denoted by the orange and blue bars, respectively. The effect that falls in between the Bonferroni and t-value limit could be considered as important. In contrast, the one that falls below the t-limit will give a negative effect, but it still can be considered to support the hierarchy. Examining this chart could reduce a false positive result or type 1 error in rejecting the null hypothesis. For this study, 5% of the error rate was assigned as an alpha in hypothesis testing. Still, when multiple tests are carried out, the chances of false-positive occurrences increase with the number of comparisons made. Bonferroni work by diving alpha to the number of testing, so the false accusation reduced with every set model. All in all, this Pareto chart agrees to the conclusion made via EDA earlier with an extra three-way interaction effect.

Table 7. FFD solution for optimization setting.

	Lower limit	Upper limit	Goal setting	Solution
X_1: Pebax concentration (wt %)	1	3	In range	3
X_2: GO dispersed in Pebax (wt %)	0	0.5	In range	0.4
X_3: GO dispersed in PSF (wt %)	0	0.4	In range	0.4
X_4: Pebax–GO coating layer	1	3	In range	1
Y: Permeate flux kg/m^{2}h	0.738569	1.03689	Maximize	1.03689 Desirability (1)

Table 8. ANOVA for optimization via CCD.

Source	Sum of squares	Degree of freedom	Mean square	*F* value	*p*-value Prob > *F*	
Model	0.099	5	0.020	29.21	0.0002	**significant**
X_1: Pebax concentration (wt %)	0.045	1	0.045	67.06	<0.0001	
X_2: GO dispersed in Pebax (wt %)	0.022	1	0.022	31.95	0.0008	
X_1X_2	3.988×10^{-3}	1	3.988×10^{-3}	5.90	0.0454	
X_1^2	0.016	1	0.016	23.93	0.0018	
X_2^2	0.015	1	0.015	22.60	0.0021	
Residual	4.728×10^{-3}	7	6.754×10^{-4}			
Lack of fit	3.185×10^{-3}	3	1.062×10^{-3}	2.75	0.1764	**not significant**
Pure error	1.543×10^{-3}	4	3.857×10^{-4}			
Correlation total	0.10	12				

Table 9. Fitting parameter for CCD.

R-Squared	0.9543
Adj R-Squared	0.9216
Pred R-Squared	0.7576
Adeq Precision	14.941

All the variables were fitted to the first-order equation (Equation 5) with permeate flux denoted by Y and X_1, X_2, X_3, and X_4 represent the Pebax concentration, GO dispersed in Pebax, GO dispersed in PSF, and coating layer, respectively.

$$Y = 0.94 + 0.025X_1 + 0.025X_2 + 0.024X_3 + 0.017X_4 - 0.017X_1X_2 + 0.011X_1X_3 - 0.010X_1X_4 - 0.026X_2X_4 - 0.025X_3X_4 + 0.017X_1X_2X_3 + 0.012X_1X_2X_4 + 0.016X_2X_3X_4 \quad (5)$$

The validity of this constructed model can be further proved by the normal probability against the plot of the studentized residuals, as illustrated in Figure 6. Almost all the internally studentized residuals lie in a straight line, which means the error term is normally distributed within the model.

The same goes for the predicted flux versus actual flux in Figure 7. This plot presents the R^2 of the model; the closeness of the data points to the fitted diagonal line illustrates a good fit [11]. An outlier could be seen

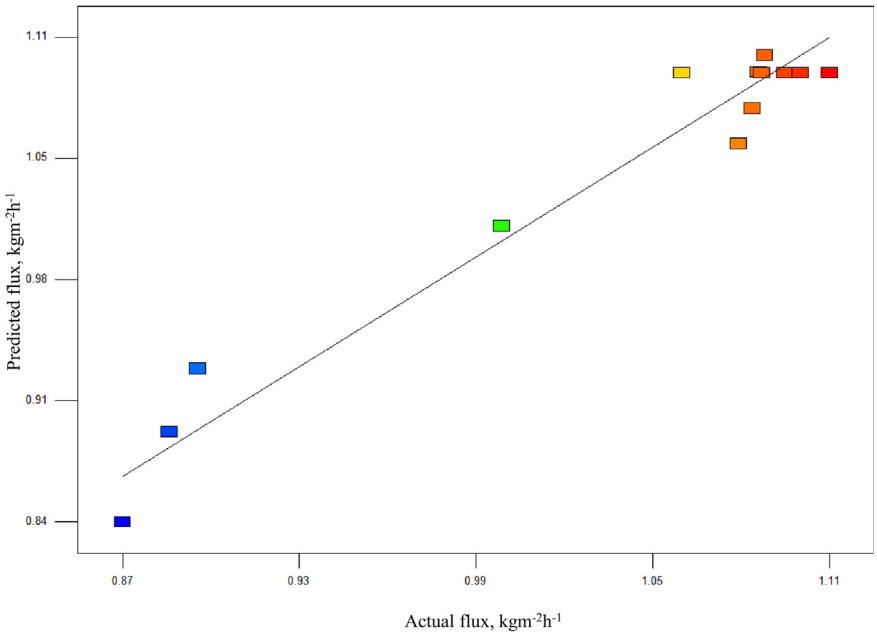

Figure 9. Predicted versus actual flux for TFNC optimization.

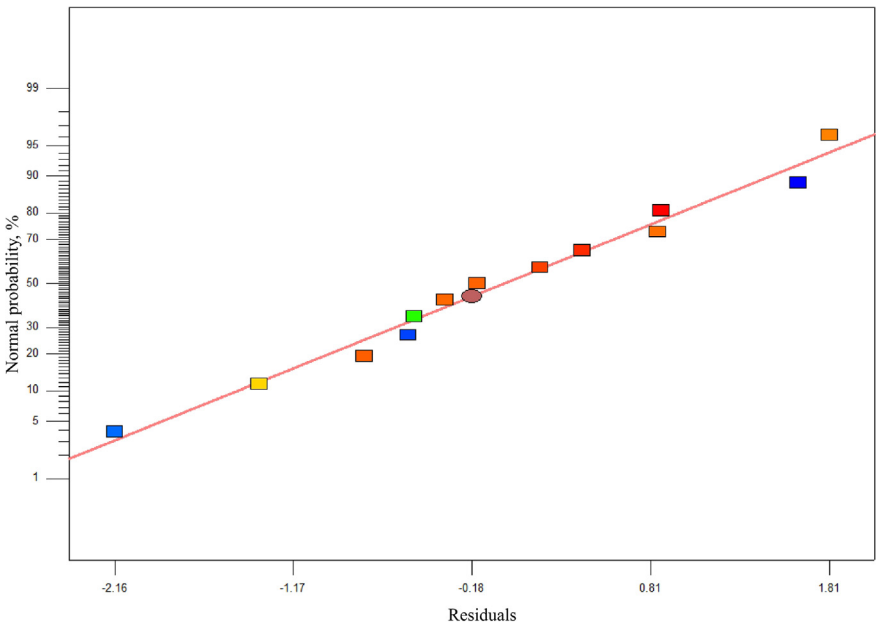

Figure 10. Normal probability plot of the residuals for flux.

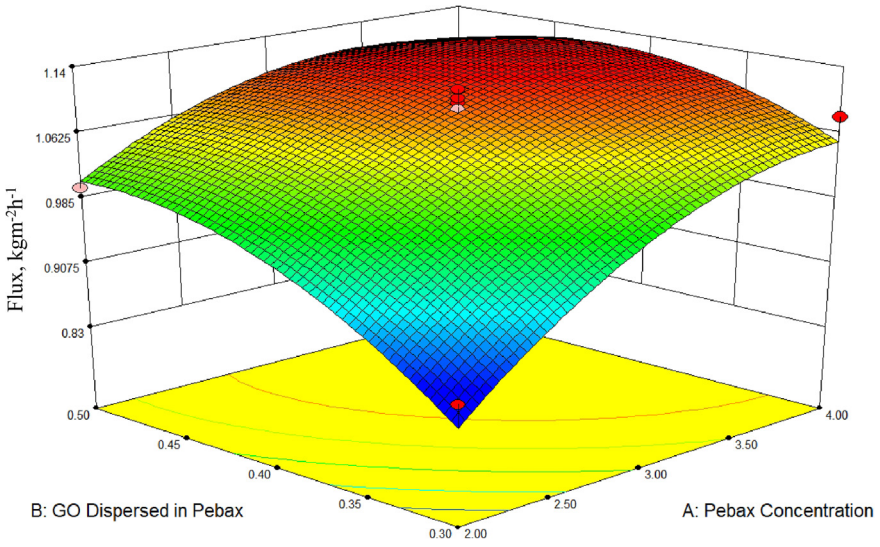

Figure 11. Response surface plot of the flux optimization.

Table 10. Model validation tests.

Run	Pebax concentration (wt %)	GO dispersed in Pebax (wt %)	Permeate flux ($kgm^{-2}h^{-1}$)		Error, %
			Predicted	Actual	
1	3.2	0.42	1.113	1.102	0.9
2	3.625	0.4725	1.120	1.131	0.9
3	3.95	0.4325	1.124	1.122	0.2
4	3.4125	0.458125	1.123	1.130	0.6
5	3.8	0.48	1.114	1.012	1.6
6	3.2972	0.42852	1.120	1.114	0.5

from these two plots, if there is any. This regression analysis happened to have no outliers making the predicted responses precise and reliable.

3.3. Interaction effect for thin film nanocomposite (TFNC) development

The two-way interaction of factors study toward permeate flux was depicted into a 3D surface plot as shown in Figure 8. Figure 8a describes the flux variation in response to the interaction of Pebax concentration (X_1) and the amount of GO loaded to the substrate layer (X_2). Permeate flux responds better to the Pebax concentration changes compared to the amount of GO loaded into it. There is an infinitesimal value of about 0.015565 $kgm^{-2}h^{-1}$ when both factors interact at the high setting of X_1 (3 wt %), while it widely deviates at a low setting (1 wt % of Pebax) as much as 0.084201 $kgm^{-2}h^{-1}$. The inconsistency of flux variation due to the changes in the parameters between low and high shows that the parameters are not complementing each other. Many studies have proved that polymer concentration plays a vital role in film development due to the direct correlation to viscosity and film morphology.

A significant finding of this composite film development was observed in the interaction of the selective layer concentration (X_1) and the amount of GO dispersed into the PSF substrate (X_3). A dynamic variation of flux responding to the changes of both factors between the setting shows a synergetic effect between the layers. Increasing X_3 from 0 to 0.4 wt % improved the permeate flux at both settings of X_1. The GO dispersed into the substrate or support layer increases the hydrophilic moieties of the TFNC and reduces the interlayer surface fouling. The presence of GO on the PSF substrate induces a more negative surface charge, which is often said as an anti-fouling resistance compared to the non-GO surface [12].

The addition of another Pebax–GO layer (X_4) did not affect much at the high setting of X_1 as can be seen in Figure 8c. This might be due to the increase in flux transfer resistance from the thicker selective layer. Comparatively, flux is much dependable toward the changes in X_4 at the lowest setting of X_1. Increasing the coating layer compensates for the inconsistency of selective layer form due to the low viscosity of Pebax solution. It was reported in several studies that it could lead to solution penetration and pore blockage that consecutively disturbs the solution diffusion mechanism [13, 14].

As for the interaction of amount of GO dispersed into the Pebax selective layer (X_2) and numbers of Pebax–GO layer (X_4) (Figure 8d), flux responds positively with the increasing selective layer when only there is no GO dispersed into the layer. So, increasing selective layer increases flux transfer resistance. However, the layer brings more water selective terminal from the polar rich PA part of the copolymer. Adding GO (X_2) to the selective layer helps in reducing the Pebax–GO layer (X_4) needed for a successful water selective separation by reducing the thickness of the selective coating. The same trend can also be observed in Figure 8e in the interaction of amount of GO dispersed in PSF support layer (X_3) and Pebax–GO selective layer (X_4). It is like a different approach to increasing the hydrophilicity of the film. In conclusion, the presence of GO in either layer resulted in a minimum selective layer coating needed for the highest permeating flux.

A set of setting concluded the screening via full factorial techniques is presented in Table 7. Based on the highest response, two factors were selected for optimization via response surface methodology: X_1 and X_2. Factors X_3 and X_4 were fixed for the entire study while the best X_1 and X_2 values were set up as center points for the RSM study (Table 4).

3.4. Design optimization via RSM approach

Table 8 presents the ANOVA results for the flux and its significant model terms, while Table 9 lists the adequacy measures of R^2, adjusted R^2, and predicted R^2. These were appeared to be high. As desired, the measured R^2 must be greater than 0.9, thus the model is statistically significant. An adequate precision ratio of 14.941 indicates good model discrimination for this design as it appeared to be greater than 4.

The Model *F*-value of 29.21 implies the model is significant. There is only a 0.02% chance that a "Model F-value" this large could occur due to noise. Values of "Prob > F" less than 0.05 indicate model terms are significant. In this case, X_1, X_2, X_1X_2, X_1^2, X_2^2 are significant model terms. The "Lack of Fit F-value" of 2.75 implies the Lack of Fit is not substantial relative to the pure error. A good model must come with a not significant lack of fit, with a *p*-value greater than 0.1. If not, the model cannot be used as a response predictor. Lack of fit statistic occurs when there is a replicator in the design space. As for this design, there are five replications of center point, where the point is directly taken from the FFD study.

Figure 9 shows the relationship between the actual and predicted values of the flux. This figure indicates that the developed model is adequate since the residuals in the prediction of each response are small, with the residuals approaching the diagonal line. Even though the residual seems to be accumulated on a specific part, it is homoscedastic, and it came from normally distributed data (Figure 10). The data distribution was reliable when it is closely distributed along the diagonal line in a residuals plot [11].

An optimum point relating X_1 and X_2 and how both factors interact to achieve a maximum flux is illustrated in Figure 11. GO interacts well with Pebax because both materials are depositing different ionic charges. The electrostatic attraction and hydrogen bonding of the two materials strengthen the dispersion for an enhanced water selective barrier [15].

A permeate model in Eq. (6) concluded this study as below.

$$\text{Permeate flux} = 1.09 + 0.075X_1 + 0.052X_2 - 0.032X_1X_2 - 0.048X_1^2 - 0.047X_2^2 \quad (6)$$

where X_1 and X_2 is the Pebax concentration and amount of GO dispersed into Pebax, respectively. A predicted and actual fluxes were compared and tabulated in Table 10. From the findings, all the runs exhibited less than 5% errors, proving that the model can predict the response excellently.

4. Conclusion

Pebax–GO–PSF TFNC was successfully developed by combining FFD and CCD for an optimum design condition to achieve the highest permeate flux for IPA dehydration via pervaporation. EDA was used as a first step in accessing all the data to ensure that the developed model is in line with the experimental data. For all the samples, no traces of alcohol were detected, making permeate a single response for the study. Among the factors studied, Pebax concentration and amount of GO dispersed into the Pebax selective layer were the most significant factors toward high permeate flux.

Declarations

Author contribution statement

Mohamad Syafiq Abdul Wahab: Conceived and designed the experiments; Performed the experiments; Analyzed and interpreted the data; Wrote the paper.

Sunarti Abd Rahman: Conceived and designed the experiments; Analyzed and interpreted the data; Contributed reagents, materials, analysis tools or data; Wrote the paper.

Rozaimi Abu Samah: Conceived and designed the experiments; Analyzed and interpreted the data; Wrote the paper.

Funding statement

This work was supported by the Ministry of Higher Education, Malaysia, with the award number RDU1901164 (FRGS/1/2019/TK02/UMP/02/17).

Data availability statement

Data will be made available on request.

Declaration of interests statement

The authors declare no conflict of interest.

Additional information

No additional information is available for this paper.

References

[1] P. Onsekizoglu, K. Savas Bahceci, J. Acar, The use of factorial design for modeling membrane distillation, J. Membr. Sci. 349 (1) (2010) 225–230.
[2] A.A. AlcheikhHamdon, N.A. Darwish, N. Hilal, The use of factorial design in the analysis of air-gap membrane distillation data, Desalination 367 (2015) 90–102.
[3] Z. Huang, et al., Poly(vinyl alcohol)/ZSM-5 zeolite mixed matrix membranes for pervaporation dehydration of isopropanol/water solution through response surface methodology, Chem. Eng. Res. Des. 144 (2019) 19–34.
[4] M. Mubashir, et al., Study on the effect of process parameters on CO2/CH4 binary gas separation performance over NH2-MIL-53(Al)/cellulose acetate hollow fiber mixed matrix membrane, Polym. Test. 81 (2020) 106223.
[5] M.B. Rosly, et al., Effect and optimization parameters of phenol removal in emulsion liquid membrane process via fractional-factorial design, Chem. Eng. Res. Des. 145 (2019) 268–278.
[6] Z.W. Song, L.Y. Jiang, Optimization of morphology and performance of PVDF hollow fiber for direct contact membrane distillation using experimental design, Chem. Eng. Sci. 101 (2013) 130–143.
[7] M. Khayet, et al., Hollow fiber spinning experimental design and analysis of defects for fabrication of optimized membranes for membrane distillation, Desalination 287 (2012) 146–158.
[8] M. Naderi, E. Khamehchi, Nonlinear risk optimization approach to water drive gas reservoir production optimization using DOE and artificial intelligence, J. Nat. Gas Sci. Eng. 31 (2016) 575–584.
[9] Abdul Wahab, M.S., S. Abd Rahman, and R. Abu Samah, Super selective dual nature GO bridging PSF-GO-Pebax thin film nanocomposite membrane for IPA dehydration. Polymer-Plast. Technol. Mater..
[10] S. Panić, et al., Optimization of thiamethoxam adsorption parameters using multi-walled carbon nanotubes by means of fractional factorial design, Chemosphere 141 (2015) 87–93.
[11] X.S. Yi, et al., Factorial design applied to flux decline of anionic polyacrylamide removal from water by modified polyvinylidene fluoride ultrafiltration membranes, Desalination 274 (1) (2011) 7–12.
[12] F. Baskoro, S. Rajesh Kumar, S. Jessie Lue, Grafting thin layered graphene oxide onto the surface of nonwoven/PVDF-PAA composite membrane for efficient dye and macromolecule separations, Nanomaterials (Basel, Switzerland) 10 (4) (2020) 792.
[13] L.-F. Liu, et al., Modification of PSf/SPSf blended porous support for improving the reverse osmosis performance of aromatic polyamide thin film composite membranes, Polymers 10 (6) (2018).
[14] T. Bucher, et al., Formation of thin, isoporous block copolymer membranes by an upscalable profile roller coating process—a promising way to save block copolymer, Membranes 8 (3) (2018).
[15] E. Halakoo, X. Feng, Layer-by-layer assembled membranes from graphene oxide and polyethyleneimine for ethanol and isopropanol dehydration, Chem. Eng. Sci. 216 (2020) 115488.